Dyes and Pigments 92 (2011) 642–653

Contents lists available at ScienceDirect

Dyes and Pigments

journal homepage: www.elsevier.com/locate/dyepig

Investigation of tensile properties and dyeing behavior of various polypropylene/polyamide 6 blends using a mixture experimental design

Saeed Asiaban, Siamak Moradian*

Department of Polymer Engineering and Color Technology, Amirkabir University of Technology, P.O. 15875-4413, Tehran, Iran

ARTICLE INFO

Article history:
Received 16 November 2010
Received in revised form
26 March 2011
Accepted 18 May 2011
Available online 29 June 2011

Keywords:
Polypropylene
Polyamide 6
Maleic anhydride polypropylene
Mixture experimental design
Disperse dye
Acid dye

ABSTRACT

Polypropylene has many advantages over other polymeric fibers such as high tensile strength, good abrasion resistance, high chemical resistance and very competitive price. However, the use of polypropylene fiber is restricted by the lack of affinity of conventional dyestuffs for this fiber. Many attempts have been made to improve the dyeability of polypropylene by various techniques. It must however, be noted that enhanced dyeability of polypropylene should not adversely impair its other properties, in particular its mechanical properties. To this end, in the present investigation, a mixture experimental design was used in order to attain an optimal region of proportions of three components namely polypropylene (PP), maleated polypropylene (polypropylene grafted with maleic anhydride (MAH-PP) as a compatibilizing agent) and polyamide 6 (PA6); where enhanced dyeability as well as retained mechanical properties would be achieved. Additionally, in order to analyze the morphology of the blends, differential scanning calorimetry (DSC) and scanning electron microscopy (SEM) were used. Finally, in order to evaluate effect of each component on fastness properties of the blends, wash, rub and light fastnesses were determined by the corresponding standard test methods.

1. Introduction

Polypropylene (PP) is a polymeric material utilized for the manufacturing of many products such as injection-molded parts, packaging films and mono-axially oriented film tapes for carpet backing and sacks [1].

Despite many advantages such as high tensile strength, good abrasion resistance, high chemical resistance, low density and low cost, the use of polypropylene fiber is restricted by the fact that most dyes lack affinity for this fiber. Therefore polypropylene isn't suitable for conventional dyeing techniques using disperse or acid dyes. Although dye affinity is strictly a thermodynamic property, dyeability is also related to kinetic factors such as crystallinity, since this is believed to reduce diffusion of a dye into the fiber matrix [2]. Many attempts have been made to improve dyeability of polypropylene. Physical modification methods are used for improving dyeability of many polymers such as polypropylene. These could be performed physically by mixing a host polymer with polymeric additives, metal compounds, low molecular weight materials and even organic or inorganic nano-materials in a batch mixer or an extruder [3–6]. Chemical modification methods are based on placement of dye receptors in the host polymeric chains via block or graft copolymerization [3]. Physical modification of polypropylene has been considered more extensive than the chemical modification counterparts. This could be due to technical feasibility and economical viability without unduly impairing other properties. Son et al. [7] have reported that a disperse dyeable polypropylene can be prepared by melt blending it with poly (ethylene-covinyl acetate) prior to extrusion. Hong et al. [8] have reported improved dyeability of polypropylene fibers using copolymer additives. The copolymer used consisted of strearyl methacrylate plus one of three additional components that conferred dye sites for acid or basic dyes or both. Dyeing tests showed that the copolymer additives improved dyeability of polypropylene. The mechanical properties of the fiber were not greatly affected by the copolymer additives. Mizutani et al. [9] have studied dyeing behavior of glycidyl methacrylate divinylbenzene modified polypropylene fiber with disperse dyes. The results showed that the fiber was well dyed in the presence of carriers. Seves et al. [10] have prepared blends of isotactic polypropylene (iPP) with hydrogenated oligocyclopentadiene (HOCP), a glassy amorphous resin, in order to make dyeable fibers from an aqueous dyebath. These fibers showed better light, wet-washing and cleaning fastness properties than iPP while retaining most of the original mechanical properties. Ujhelyiova et al. [11] have prepared polypropylene/polyester (PP/PES) blends for improving dyeability of PP fibers. Polyester addition in the PP matrix

* Corresponding author. Tel.: +98 21 64542425; fax: +98 21 88080871.
E-mail address: moradian@aut.ac.ir (S. Moradian).

0143-7208/$ – see front matter © 2011 Elsevier Ltd. All rights reserved.
doi:10.1016/j.dyepig.2011.05.019

increased uptake of dyes from a dyebath. They have presented the influence of two polyesters in dyeing kinetics of PP/PES blend fibers by the disperse dye C.I. Disperse Blue 56 (Terasil Blue 3RL).

The use of amine derivatives could be a suitable approach for modifying polypropylene in order to dye with acid and disperse dyes. Kotek et al. [2] have studied dyeing behavior of three disperse dyes on an alloy fiber composed of polypropylene and polyamide 6 (PA6) produced by melt spinning. Akraman et al. [12–15] have synthesized two amine polymeric compounds so that after blending with polypropylene improved dyeability with acid dyes could be encountered. They have evaluated kinetic and thermodynamic parameters of the dyeing system, ionic exchange mechanism of dyeing and effect of drawing on dyeability of the modified polypropylene fibers. Seves et al. [16] have studied dyeing characteristics of PP/PA6 fiber blends. They showed that the fiber was easily dyeable with disperse dyes and wash and dry cleaning fastnesses were quite satisfactory. Amongst amine derivatives, polyamide 6 is one of the major materials capable of improving the dyeing of polypropylene with disperse dyes. As PP/PA6 blends are strongly incompatible, the use of an appropriate interfacial agent or compatibilizing agent (commonly referred to in the literature as a compatibilizer) is needed in order to obtain good interfacial adhesion and a better dispersion of the polyamide particles within the PP matrix [16].

It is important to note that enhanced dyeability of polypropylene should not adversely impair its mechanical properties. Therefore, it is necessary to prevent loss of mechanical properties of polypropylene during any process in which enhanced dyeability is sought after. Enhanced dyeability without impairing mechanical properties must make use of methods in which optimization between enhanced dyeability and mechanical properties are guaranteed. One such method is often used when the response (i.e. enhanced dyeability or a mechanical property) is a function of proportions of each component within a blend is the mixture experimental design.

In the present paper use is made of a mixture experimental design in order to attain an optimal region of proportions of the three components (i.e. PP/MAH-PP/PA6) in which enhanced dyeability (represented by the Kubelka–Munk (K/S) ratio) is achieved together with retained mechanical properties (represented by the tensile strength and the elongation at break). Finally, the effect of each component on wash, rub and light fastness properties of the blends was evaluated.

2. Mixture experimental design

Mixture experimental design is a special class of response surface representing various mixture models which depict suitable correlation between the response under investigation and the proportions of the components. For three component mixtures, four types of models could be fitted for a particular response. These models include: linear, quadratic, special cubic and full cubic models. The lowest-order model for a three component mixture design is a linear model as shown in equation (1) by which the response (Y) is linearly correlated with proportions (i.e. β_1, β_2 and β_3) of the three components (i.e. X_1, X_2 and X_3). In order to fit this model, it is necessary to determine the three coefficients β_1, β_2 and β_3. For this purpose, at least three experimental data is required. Also, to establish the validity of the fitted model, it is necessary to measure the response (Y) at other proportions of the components.

$$Y = \beta 1X1 + \beta 2X2 + \beta 3X3 \quad (1)$$

If a higher-order relationship is suspected, then more experiments must be carried out because there will be more coefficients in the model due to interactions between the components' proportions [17]. The highest-order model for a three component mixture design would be a full cubic model which would have ten coefficients as shown in equation (2):

$$\begin{aligned} Y = {} & \beta 1X1 + \beta 2X2 + \beta 3X3 + \beta 1\beta 2X1X2 + \beta 1\beta 3X1X3 \\ & + \beta 2\beta 3X2X3 + \beta 1\beta 2\beta 3X1X2X3 + \beta 1,2X1X2(X1 - X2) \\ & + \beta 1,3X1X3(X1 - X3) + \beta 2,3X2X3(X2 - X3) \end{aligned} \quad (2)$$

This full cubic model contains three linear terms related to the three components, three quadratic terms for the three 2-way interactions and four cubic terms for the four 3-way interactions. Therefore, at least ten experimental data for fitting the model would be required. Also, further experimental data are necessary to establish the validity of the fitted model. It is important to always initially consider maximum order required for the fitted model so as to be able to adequately model the response surface. Mixture experiments frequently require a higher-order model than is initially planned. Therefore, it is usually a good idea, whenever possible to perform additional runs beyond the minimum required to fit the model [18]. Therefore, for a three component mixture design, the number of test runs of highest possible should be considered for fitting a full cubic model. After performing the experimental test runs and determining the coefficients of the full cubic model, the fitted model may have some insignificant coefficients for the 2- and 3-way interactions which did not influence the response variation so they can be removed from the fitted model. Removing the insignificant coefficients and reducing the model allows us to simplify a regression model and can make the model easier to work with and yet maintain its high accuracy. Presence of insignificant coefficients in the model may impair the model's predictive ability. A model can be reduced manually, or automatically using an algorithmic procedure, such as a stepwise regression, which is suggested by the mixture experimental design software. In the present investigation, creating and analyzing the mixture design and also plotting the results were performed by Minitab® 15 software presented by Minitab Incorporation. The software performs the Student's t-test and calculates a p-value for each coefficient of the 2- and 3-way interactions. P-value is a suitable criterion for determining which coefficient of the 2- and 3-way interactions is statistically insignificant and should be removed from the model. P-value determines the appropriateness of rejecting the null hypothesis in a hypothesis test. Hypothesis test is a procedure that evaluates two mutually exclusive statements about a population. A hypothesis test uses sample data to determine which statement is best supported by the data. These two statements are called the null hypothesis and the alternative hypotheses. In order to approve the significance of a coefficient, the null hypothesis which explains the coefficient is zero (or is not significant) must be rejected. For this purpose, the p-value must be less than or equal to a significant level or α-level. Alpha (α) is the maximum acceptable level of risk for rejecting a true null hypothesis and is expressed as a probability ranging between 0 and 1. If the p-value is less than or equal to the α-level, reject the null hypothesis in favor of the alternative hypothesis i.e. the coefficient is significant. But if the p-value is greater than the α-level, fail to reject the null hypothesis. The most commonly used α-level is 0.05. At this level, the chance of finding an effect due to the coefficient-related interaction that does not really exist is only 5%. Therefore, if the p-value is greater than the α-level, the model should be reduced by removing the insignificant coefficient. After removing the first insignificant coefficient, the regression could be repeated so that each time one insignificant coefficient is removed, until only statistically significant coefficients remain. On the other hand,

Percentage of response variation which is explained by its relationship to one or more component variables, could be adjusted for each variable in the model. This adjustment is important because square of correlating coefficient (R^2) will always increase when a new term is added to any model. A model with more terms may appear to have a better fit simply because it has more terms. But the adjusted R^2 will only increase if the new term improves the model more than would be expected by chance. Therefore, if adjusted R^2 decreases while reducing the model it is recommended that the coefficient should not be removed from the model. However, it is necessary to evaluate goodness-of-fit of the reduced model. To perform additional runs beyond the minimum required to fit the model permits establishing the validity of the fitted model. In this state, there are two experimental data groups. The first group is used to fit the regression model and the second group includes experimental data which are used to evaluate residuals error of the fitted model. Sum of squares (SS) parameter is the sum of squared residuals. Regression-related SS parameter is the portion of the variation explained by the fitted model, while residual error-related SS parameter is the portion not explained by the fitted model and is attributed to error. Degree of freedom (DF) indicates the number of independent pieces of information involving the response data needed to calculate the mean square (MS) parameter. If n = number of the experimental data and p = number of the terms in the fitted model, regression-related $DF = p - 1$ and residual error-related $DF = n - p$. MS parameter is calculated via dividing SS by DF. Therefore, two MS parameters can be defined for the regression model and the residual error. The adequacy (significance) of the model is determined by performing the Fisher test which results in calculation of the F-value. The regression-related F-value is calculated via dividing MS for regression by MS for residual error. Larger values of F support rejecting the null hypothesis that there is not a significant model. If the F-value is greater than the $F_{(DF1,DF2)}$ value, the model will be adequate for explaining the response variations. In this condition, p-value is less than α-level (i.e. 0.05). The $F_{(DF1,DF2)}$ value is determined by the F distribution tables. DF1 and DF2 are degrees of freedom of a numerator and a denominator, respectively. For the F distribution tables, the rows represent the denominator degrees of freedom and the columns represent the numerator degrees of freedom [19]. In this state, DF1 and DF2 are degrees of freedom of the regression model and the related residual error, respectively. In addition to the regression F-value, the F-value for the lack-of-fit is a criterion for evaluating adequacy (significance) of the fitted model. If n = number of the replicated experimental data and m = number of the experimental data for the residual error, the pure error $DF = n - 1$ and the lack-of-fit $DF = m - n - 1$. Therefore, two MS parameters can be defined for the lack-of-fit and the pure error (noise). The F-value for the lack-of-fit is calculated via dividing MS for the lack-of-fit by MS for the pure error. If the F-value for the lack-of-fit is less than the $F_{(DF1,DF2)}$ value, it will indicate an adequate goodness-of-fit. Also, if significant level is 0.05, p-value will be larger than it. Similarly, the $F_{(DF1,DF2)}$ value is determined by the F distribution tables. Here, DF1 and DF2 are degrees of freedom of the lack-of-fit and the pure error, respectively [20].

It is important to note that the residuals will be distributed normally if the model indicates an adequate goodness-of-fit. For this purpose, the normality test could be performed through calculating Anderson–Darling statistic by Minitab® 15 software. The Anderson–Darling statistic measures how well the residuals follow a particular distribution e.g. a normal distribution. The better the distribution fits the data, the smaller this statistic will be. In practice, this test compares the empirical cumulative distribution function of the residuals with the distribution expected if the data were normal. If this observed difference is sufficiently large, the test will reject the null hypothesis (H_0) of population normality. The hypotheses for the Anderson–Darling test are H_0: the residuals follow a normal distribution and H_1: the residuals do not follow a normal distribution. If the p-value for the Anderson–Darling test is lower than the chosen significance level (usually 0.05), conclude that the data do not follow the normal distribution. Sometimes the software may not display a p-value for the Anderson–Darling test because it may not mathematically exist for certain cases. In the present paper, the software calculated the p-value for the residuals related to the fitted models. Therefore, the normality test generates a normal probability plot and performs a hypothesis test to examine whether or not the residuals follow a normal distribution. Along with probability plot of the residuals, the test displays a table with distribution parameter estimates, the Anderson–Darling statistic and related p-value in order to evaluate the distribution fit to the data [19,20].

3. Experimental

3.1. Mixture design suggested samples

In order to create a mixture design, type of design, number of components, degree of design, number of points required to achieve the best model, replication points, name of components and their upper and lower limits must be entered into the software. In the present investigation, the three used components were PP V30S (PP), Akulon F130 (PA6) and Fusabond® P MD353D (MAH-PP) and their respective lower and upper limits of proportions were 0.7 to 1, 0 to 0.3 and 0 to 0.15. According to such limits, the type of design was an extreme vertices design which is one of three design types the software can create for three component mixtures. By selecting a design degree of 3 (the highest possible order of the design) and augmenting the center and axial points (the additional test runs), the software suggested 13 points for experimentation. Also, in order to provide an estimate of the experimental error or noise in the process and achieve more precise estimates of the components effect, the center point was replicated twice. Therefore, in total the software suggested 15 test samples the proportions of which are shown in Table 1. It must be remembered that the sum of the proportions of the components for each sample is always 1. Fig. 1 shows the extreme vertices design space which is highlighted in grey color. Incidentally, the 15 experimental test points provided adequate data for fitting and validating a full cubic regression model.

Table 1
Mixture design suggested samples.

Sample number	Proportion of the components		
	PP	MAH-PP	PA6
1	0.8125	0.075	0.1125
2	0.925	0.075	0
3	0.85	0.15	0
4	1	0	0
5	0.75625	0.0375	0.20625
6	0.7	0.15	0.15
7	0.7	0.075	0.225
8	0.90625	0.0375	0.05625
9	0.85	0	0.15
10	0.83125	0.1125	0.05625
11	0.775	0.15	0.075
12	0.75625	0.1125	0.13125
13	0.7	0	0.3
14	0.8125	0.075	0.1125
15	0.8125	0.075	0.1125

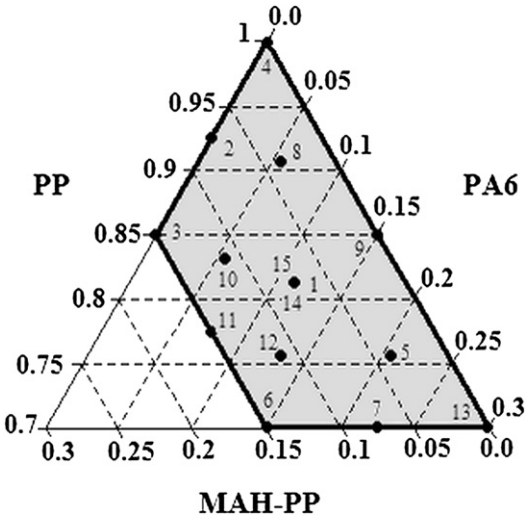

Fig. 1. The extreme vertices design space.

3.2. Materials

Fiber grade isotactic polypropylene, known as Moplen V30S, supplied by the Iranian Arak petrochemical company was used. This polymer had a melt flow index (MFI) of 18 g/10 min and density of 0.92 g ml^{-1}. Fiber grade polyamide 6 (PA6), known as Akulon F130, was obtained from the DSM company. This polymer was a medium viscosity polyamide having a viscosity number of 197 ml g^{-1} (ISO 307), melting point of 220 °C, density of 1.13 g ml^{-1} and amine content of 38 meq kg^{-1}. Maleic anhydride grafted polypropylene; Fusabond® P MD353D was supplied by the Dupont company which was used as a compatibilizer. This material had melting temperature of 136 °C and MFI of 450 g/10 min (190 °C/2.16 kg). The grafting level of maleic anhydride was very high. Disperse and acid dyes used in this work were C.I. Disperse Yellow 3 (Cibacet Yellow 2GC) and C.I. Acid Yellow 110 (Polar Yellow 5GN), respectively, supplied by the Ciba company. The disclosed chemical structure of the disperse dye is given in Fig. 2.

3.3. Sample preparation

Akulon F130 and Fusabond® P MD353D were first dried at 80 °C for 16 h to ensure the removal of residual moisture. After drying, PP V30S and Fusabond® P MD353D were melt blended in a batch mixer brabender® plasticorder® W50 at 190 °C and 60 rpm for 1 min. Then, the temperature of the batch mixer was automatically increased from 190 °C to 240 °C during 2 min. When the temperature was fixed at 240 °C, Akulon F130 was added to the mixer. The mixing operation was continued for one further minute after the mixer torque became constant. The total time of the blending process time was approximately 8 min for each sample. After blending, the samples were dried at 80 °C for 16 h in order to remove any absorbed moisture. Immediately, the samples were molded by a compression molding machine i.e. the Dr Collin PCS II P 400P® at 1.5 MPa and 190 °C in order to prepare films of 150 μm thicknesses ready for tensile measurements and dyeing with the selected dyes. Additionally, samples of 2 mm thickness were prepared under the same conditions for morphology evaluation by scanning electron microscopy (SEM).

In order to compare the dyeing behavior of various samples to that of the pure polyamide 6, it was necessary to prepare Akulon F130 films of 150 μm thickness in a similar manner. For this purpose, Akulon F130 was dried at 80 °C for 16 h and then molded by the compression molding machine at 1.5 MPa and 240 °C.

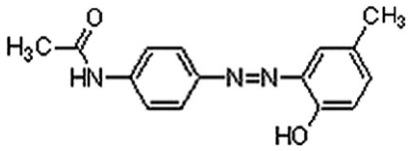

Fig. 2. Chemical structure of C.I. Disperse Yellow 3.

3.4. Dyeing

3.4.1. Disperse dyeing

The prepared film samples for the dyeing process had the dimensions of 3 cm × 3 cm × 150 μm. The dye concentration in the dyebath was 3% w/w (weight of dye per weight of film) and the liquor to goods ratio was 100:1. pH of the dyebath was 5 to 5.5 through addition of acetic acid. Eriopon OL was used in an amount of 0.5% w/w in order to improve dispersion of dye particles in the bath. Each sample was added to the prepared dyebath at room temperature. Then the temperature was raised to the boiling point (BP) at a rate of 2 °C min^{-1}. The dyeing process was continued for a further 60 min at boil. Fig. 3 shows the temperature profile of the dyeing process. In order to remove excess dye precipitated on the surface of the dyed film, a reduction clear process was performed after the dyeing process. The reduction clear bath had 2 g l^{-1} of sodium hydroxide, 3 g l^{-1} of sodium hydrosulfite and 2 g l^{-1} of a detergent with a liquor to goods ratio of 100:1. The process was performed at 70 °C for 20 min.

3.4.2. Acid dyeing

Film dimensions, acid dye concentration and liquor to goods ratio for the acid dyeing process were exactly like those for the disperse dyeing process. pH of the dyebath was 4.5 which was adjusted with acetic acid. Ammonium sulfate was used in an amount of 1 g l^{-1}. Similar to the disperse dyeing, the dyebath temperature was raised to the boiling point (BP) at a rate of 2 °C min^{-1} and the dyeing process continued for a further 60 min at the boil.

3.5. Spectrophotometry

Reflectance curves ($R_\infty(\lambda)$) of the dyed samples were measured on a Gretag Macbeth® spectrophotometer 7000A. These reflectance were converted to the corresponding Kubelka–Munk ratio $(K/S)_\lambda$ of the one constant theory by the use of equation (3).The maximum values of K/S at λ_{max} 420 nm (since the dye was yellow) were used as a criterion for dye uptake.

$$(K/S)_\lambda = (1 - R_\infty(\lambda))^2 / 2R_\infty(\lambda) \quad (3)$$

3.6. Tensile measurement

According to the ASTM D882 standard recommended for measuring tensile properties of polymeric films, the film samples

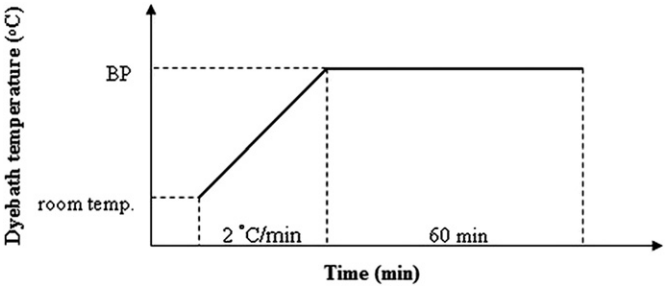

Fig. 3. Temperature profile of the dyeing process.

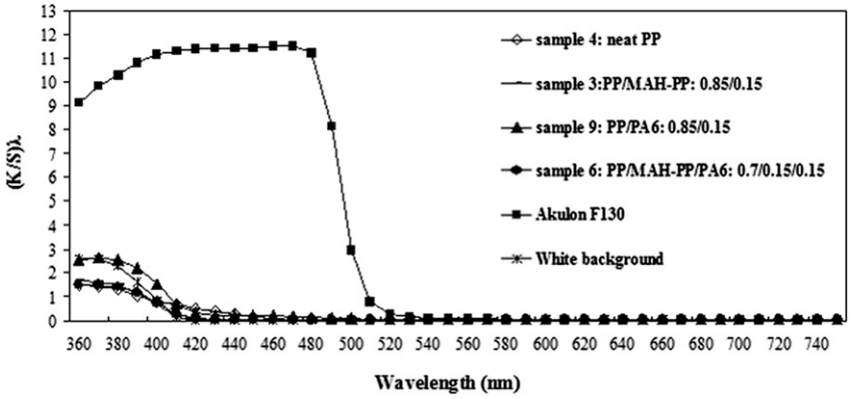

Fig. 4. The $(K/S)_\lambda$ curves of some acid dyed samples.

were cut to the required dimensions having thicknesses of 150 μm. Tensile testing was performed by a Gotech® universal testing machine AL-700 LA5 after conditioning the test samples at 23 ± 2 °C and $50 \pm 5\%$ relative humidity for 24 h. In this investigation, the average value of tensile strength and elongation at break for three replicate samples are reported.

3.7. Scanning electron microscopy (SEM)

In order to evaluate morphology of the samples scanning electron microscopic (SEM) images were taken by VEGA\\TESCAN scanning electron microscope operated at 20 kV with 15 kx magnification. For this purpose, the samples were broken under liquid nitrogen and etched by formic acid (96%) for 4 h. SEM images were taken from fracture surface of the samples which were coated with gold.

3.8. Differential scanning calorimetry (DSC)

After drying the samples at 80 °C for 16 h for the removal of absorbed moisture, differential thermal analysis of the samples was carried by a Mettler-Toledo® DSC 822 instrument. The samples were heated from 25 °C to 250 °C at a scanning rate of 10 °C min^{-1} (run 1) in order to remove thermal history induced by previous processes. Then the samples were cooled down to 25 °C (run 2). Again, the samples were re- heated from 25 °C to 250 °C at the same scanning rate (run 3).

3.9. Assessment of fastness properties

In order to evaluate the effect of each component on fastness properties of the blends, wash, rub and light fastnesses were determined by the corresponding standard test methods namely: ISO/R 105/IV, Part 9, ISO/R 105/I, Part 18 and ISO/R 105/V, Part 2, respectively. The test results were assessed by the gray scale for the wash and the rub fastnesses and the blue scale for the light fastness.

4. Results and discussion

4.1. Acid and disperse dye uptakes

In order to determine the maximum values of K/S (or K/S_{max}), it is necessary to determine the reflectance data of the dyed samples. For this purpose, each sample was placed on a white background and then its reflectance data were determined by the spectrophotometer. Also, the reflectance data of the white background were measured by the spectrophotometer. After determining the reflectance data of the dyed samples, they were converted to the corresponding Kubelka–Munk ratio $(K/S)_\lambda$ of the one constant theory. Figs. 4 and 5 show $(K/S)_\lambda$ curves of some acid or disperse dyed samples, respectively . Then K/S_{max} values were determined at λ_{max} equal to 420 nm. Table 2 shows K/S_{max} values for acid and disperse dyed samples together with a dyed pure Akulon F130 (i.e. pure PA6) sample. According to these values, disperse dye uptakes of most blend samples are high, to the extent that some equal that for the pure polyamide (i.e. Akulon F130) sample. Despite high disperse dye uptake of most blended samples, as expected, the acid dye uptake of all samples were unacceptable their K/S_{max} values being always less than 1. The K/S_{max} value for the acid dyed Akulon F130 sample was 11.38 i.e. at least 11 times more than that for the acid dyed samples. In principle, acid dyes are anionic water-soluble dyes which migrate from

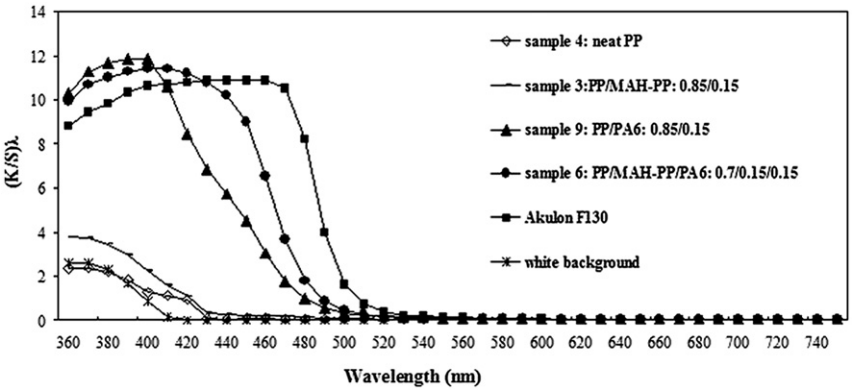

Fig. 5. The $(K/S)_\lambda$ curves of some disperse dyed samples.

Table 2
Experimental K/S_{max} values for acid and disperse dyed samples.

Samples	Proportion of the components			K/S_{max}	
	PP	MAH-PP	PA6	Acid dyeing	Disperse dyeing
1	0.8125	0.075	0.1125	0.046	8.726
2	0.925	0.075	0	0.803	1.040
3	0.85	0.15	0	0.853	1.060
4	1	0	0	0.519	0.948
5	0.75625	0.0375	0.20625	0.758	12.495
6	0.7	0.15	0.15	0.084	11.174
7	0.7	0.075	0.225	0.978	11.719
8	0.90625	0.0375	0.05625	0.052	5.385
9	0.85	0	0.15	0.334	8.458
10	0.83125	0.1125	0.05625	0.056	5.676
11	0.775	0.15	0.075	0.100	7.400
12	0.75625	0.1125	0.13125	0.068	9.621
13	0.7	0	0.3	0.159	10.805
Akulon F130				11.38	10.80

an aqueous dye bath and diffuse into the polymer matrix so that their fixation to the substrate depends strongly on ionic interaction between anionic groups of the dye and cationic dye sites in the polymer chains. For this purpose, amine modifiers which have basic nitrogen groups supply acid dye sites to interact with acid or anionic dyes in an aqueous solution. It is very important to consider that improving the acid dyeability of polypropylene depends on the amine content, the basicity of the amine's nitrogen and the molecular weight of the polyamide incorporated into the PP matrix. The more basic the nitrogen of the amine, the lesser would be the required amount of the amine modifier for incorporation into the PP matrix [12]. Considering the literature, it could be concluded that dyeing of polypropylene with acid dyes will be more feasible and efficient if the incorporated amine modifiers have low molecular weight with highly basic nitrogen content. Since Akulon F130 has an amine content of 38 meq kg^{-1} it would not be expected to enhance the acid dye uptake of such blended samples. On the other hand, Akulon F130, as a polyamide 6, is not only capable of improving the dyeing of polypropylene with disperse dyes [2,10,12–16] but it greatly improves the mechanical properties of such blends. The K/S_{max} values of acid dyed samples were only included for quantitative comparison and such values were not considered further for attaining the optimal region of proportions of the three components in which enhanced dyeability together with retained mechanical properties could be achieved.

4.2. Estimated regression models

Table 3 indicates a comparison between the experimental and fitted values of responses namely, tensile strength, elongation at break and disperse dyeing related K/S_{max} values.

By reducing equation (2), a quadratic, a partial full cubic and a quadratic models with adequate goodness-of-fit were obtained for the three responses i.e. tensile strength ($Y1$), elongation at break ($Y2$) and K/S_{max} ($Y3$) as shown in equations (4)–(6), respectively.

$$Y1 = 20X1 - 349.2X2 + 2X3 + 477.8X1X2 + 474.9X2X3 \quad (4)$$

$$Y2 = 2.4X1 - 126.1X2 - 0.8X3 - 159.6X1X2 + 201.2X2X3 + 549.1X2X3(X2 - X3) \quad (5)$$

$$Y3 = 1.1X1 + 164.8X2 - 67.6X3 - 185.7X1X2 + 147.7X1X3 \quad (6)$$

It must be remembered that $X1$, $X2$ and $X3$ represent the proportions of each component in the mixture i.e. PP, MAH-PP and PA6, respectively. Tables 4 and 5 indicate the estimated regression coefficients for the above equations and ANOVA table at 95% confidence level, respectively.

In the tensile strength regression model, there are two significant 2-way interactions in the model because the p-value of their coefficients is less than 0.05 (α-level). Because these have the same p-values therefore, both interactions have the same significant effect. The suggested model for the tensile strength variations was adequate because not only F-value for the regression model = 26.72 > $F_{tab.}$ (4, 10) = 3.48 and its p-value was less than 0.05 but also F-value for the lack-of-fit = 0.56 < $F_{tab.}$ (8, 2) = 19.37 and its p-value of lack-of-fit was greater than 0.05. Also, according to Fig. 6, the residuals distribution is normal because the p-value for the normal distribution of the residuals is 0.527 (i.e. greater than 0.05). This indicates that the tensile strength model has an adequate goodness-of-fit.

In the elongation at break regression model, although p-value of 3-way interaction was more than 0.05 but to remove the related coefficient caused a reduction in the adjusted R^2 value. Therefore, it is better to retain this coefficient in the model. Anyway, the smaller the p-value, the more significant is the corresponding coefficient [21,22]. Thus the significant effect of the interactions was ranked as: MAH-PP*PA6 > PP*MAH-PP > MAH-PP*PA6*(MAH-PP − PA6). The suggested model was adequate because F-value for the regression model = 6.61 > $F_{tab.}$ (5, 9) = 3.48 and its p-value was less than 0.05 and also F-value for the lack-of-fit = 1.03 < $F_{tab.}$ (7, 2) = 19.35 and its

Table 3
Comparison of experimental (Expl.) and predicted (Fitted) values for tensile strength, elongation at break and K/S_{max}.

Sample number	Proportion of the components			Tensile strength (MPa)		Elongation at break (%)		K/S_{max}	
	PP	MAH-PP	PA6	Expl.	Fitted	Expl.	Fitted	Expl.	Fitted
1	0.8125	0.075	0.1125	23.046	23.408	4.330	3.648	8.726	7.870
2	0.925	0.075	0	25.613	25.455	3.296	3.829	1.040	0.532
3	0.85	0.15	0	25.196	25.543	3.656	3.473	1.060	2.011
4	1	0	0	19.703	19.992	2.450	2.389	0.948	1.143
5	0.75625	0.0375	0.20625	20.133	19.665	2.106	2.283	12.495	10.880
6	0.7	0.15	0.15	23.560	22.780	4.266	3.932	11.174	11.392
7	0.7	0.075	0.225	20.707	21.361	2.396	2.425	11.719	11.470
8	0.90625	0.0375	0.05625	22.223	22.378	2.966	3.220	5.385	4.632
9	0.85	0	0.15	17.870	17.295	2.116	1.912	8.458	9.668
10	0.83125	0.1125	0.05625	27.233	25.141	5.046	4.155	5.676	5.227
11	0.775	0.15	0.075	22.870	24.161	3.473	4.166	7.400	7.532
12	0.75625	0.1125	0.13125	24.066	23.768	3.350	3.920	9.621	9.395
13	0.7	0	0.3	14.493	14.599	1.370	1.435	10.805	11.548
14	0.8125	0.075	0.1125	21.433	23.408	3.233	3.648	6.521	7.870
15	0.8125	0.075	0.1125	24.210	23.408	4.023	3.648	8.006	7.870

Table 4
Estimated regression coefficients for various regression models.

Terms of the models	Tensile strength model		Elongation at break model		K/S_{max} model	
	Coefficients	*p*-value	Coefficients	*p*-value	Coefficients	*p*-value
*X*1	20	–	2.4	–	1.1	–
*X*2	−349.2	–	−126.1	–	164.8	–
*X*3	2	–	−0.8	–	−67.6	–
*X*1*X*2	477.8	0.003	−159.6	0.05	−185.7	0.010
*X*2*X*3	474.9	0.003	201.2	0.027	–	–
*X*1*X*3	–	–	–	–	147.7	0.004
*X*2*X*3 (*X*2−*X*3)	–	–	549.1	0.085	–	–

p-value of lack-of-fit was more than 0.05. As seen in Fig. 7, the *p*-value for normal distribution of the residuals is 0.958 (i.e. greater than 0.05), so the suggested model has an adequate goodness-of-fit.

In the K/S_{max} regression model, the interaction effect related to *X*1*X*3: PP*PA6 was more significant than *X*1*X*2: PP*MAH-PP. Because *F*-value for the regression model = 53.27 > $F_{tab.}$ (4, 10) = 3.48 and *p*-value = 0 < 0.05 and also *F*-value for the lack-of-fit = 0.67 < $F_{tab.}$ (8, 2) = 19.37 and the *p*-value = 0.717 > 0.05, the suggested model was adequate. Also, according to Fig. 8, the suggested model has an adequate goodness-of-fit because the *p*-value is 0.828 (i.e. greater than 0.05) in the normality test.

Minitab® software can display the three-dimensional relationship in two dimensions via contour plotting. This plot shows how a response variable relates to three components based on a related model in two dimensions. Figs. 9–11 indicate contour plots of tensile strength, elongation at break and K/S_{max} models.

Also, the software is capable of overlaying (superimposing) the contour plots, simultaneously. Overlaid contour plots are used to visually identify the optimum region of multiple responses in a mixture experimental design [19]. According to Fig. 12, overlaying the three above mentioned contour plots illustrates an optimum region in which PP/PA6 blends have acceptable disperse dye uptake (i.e. equal to or more than that of the pure nylon 6 sample) together with minimal impairment of mechanical properties (i.e. tensile strength > 19.9 MPa and elongation at break > 2.38%). It must be remembered that cost considerations are of utmost importance; therefore linear contour plots of the cost of dyeable polypropylene can be overlaid in the optimum region to attain an optimal region of high performance/low cost dyeable polypropylene.

4.3. Morphological and thermal analyses

According to the overlaid counter plot, some interesting blends are located in the optimum region. For example, sample 6 (PP/MAH-PP/PA6: 0.7/0.15/0.15) which is located in the optimum region, has a tensile strength of 22.78 MPa (>19.9 MPa), an elongation at break of 3.93% (>2.38%) and a K/S_{max} of 11.39 (>10.8). On the other hand sample 9 (PP/PA6: 0.85/0.15) does not fall in the optimal region because its tensile strength, elongation at break and K/S_{max} are 17.29 MPa (<19.9 MPa), 1.91% (<2.38%) and 9.67 (<10.8),

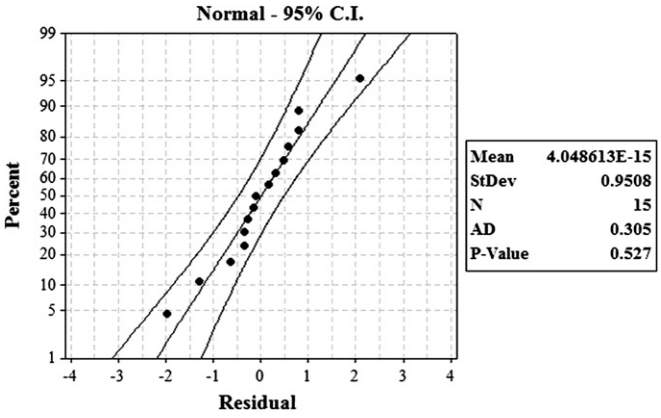

Fig. 6. Probability plot of the residuals for the tensile strength model.

respectively do not satisfy the minimum requirements. Fig. 13 compares tensile strength, elongation at break and K/S_{max} of three samples namely, sample 4 (the neat PP sample), sample 9 (PP/PA6: 0.85/0.15) and sample 6 (PP/MAH-PP/PA6: 0.7/0.15/0.15).

The tensile strength regression model reveals that the compatibilizer i.e. maleic anhydride grafted polypropylene plays an important role in improving tensile strength of the blends. In other words, at a constant proportion level of PP or PA6, the tensile strength of the blends will increase as the amount of compatibilizer is increased. As Fig. 13 shows, adding PA6 to PP by an amount of 15% (sample 9), causes a decrease in the tensile strength from 19.9 MPa for sample 4 to 17.29 MPa for sample 9. On the other hand, addition of 15% of the compatibilizer increases the tensile strength to 22.78 MPa for sample 6. Immiscibility of polypropylene and polyamide 6 is due to considerable differences in their polarities. Polymers with different polarities tend to separate and those with similar polarities tend to agglomerate, hence separate phases are formed when they are mixed. Even at the interface, they tend to reject each other (positive enthalpy), giving a weak interface which can not resist applied stress (low strength, elongation and impact strength) [23]. High surface tension of polyamide 6 causes unsuitable wetting of its particles by polypropylene. Therefore possible defects such as voids are formed at the interface which could contribute to the lowering of tensile strength [2,24]. It has been reported that the presence of a compatibilizer leads to a significant lowering of the surface tension of polyamide 6 [10,25]. Reducing the interfacial tension causes good wetting and better dispersion of the polyamide 6 particles within the PP matrix. Improving dispersion of the particles increases the surface area of polyamide 6 and this in turn promotes interaction between polyamide 6 and the compatibilizer i.e. reaction between NH2 and MAH groups, which results in formation of amide or imide linkages [25–27]. Finer dispersion of the polyamide 6 particles and formation of amide or imide linkages guarantee improvements in the tensile strength of the compatibilized blends. As Fig. 14 shows, adding 15% of

Table 5
ANOVA table for the regression models.

Source	Tensile strength model				Elongation at break model				K/S_{max} model			
	DF	*F*	$F_{tab.}$	*p*-value	DF	*F*	$F_{tab.}$	*p*-value	DF	*F*	$F_{tab.}$	*p*-value
Regression	4	26.72	3.48	0.0	5	6.61	3.48	0.008	4	53.27	3.48	0.0
Residual error	10				9				10			
Lack-of-fit	8	0.56	19.37	0.77	7	1.03	19.35	0.57	8	0.67	19.37	0.72
Pure error	2				2				2			
Total	14				14				14			

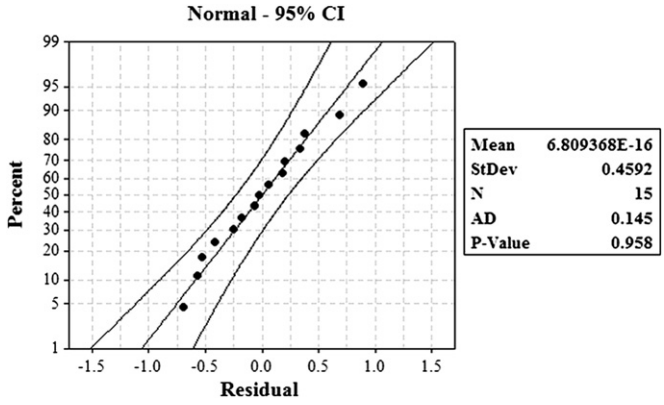

Fig. 7. Probability plot of the residuals for the elongation at break model.

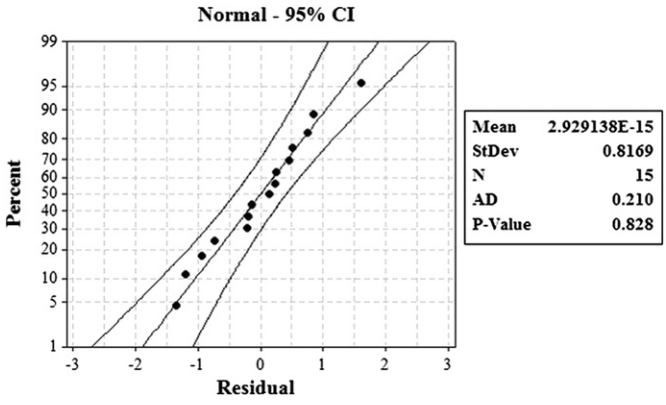

Fig. 8. Probability plot of the residuals for the K/S_{max} model.

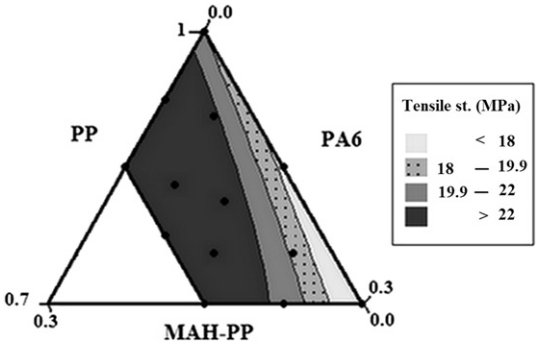

Fig. 9. Contour plot of the tensile strength model.

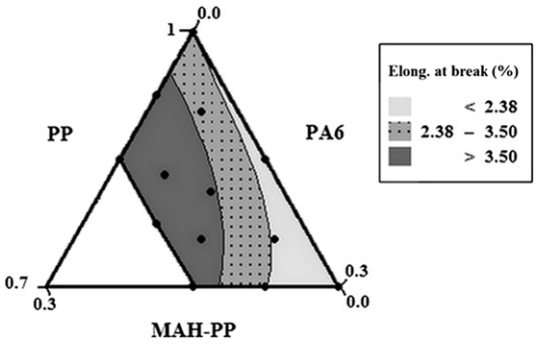

Fig. 10. Contour plot of the elongation at break model.

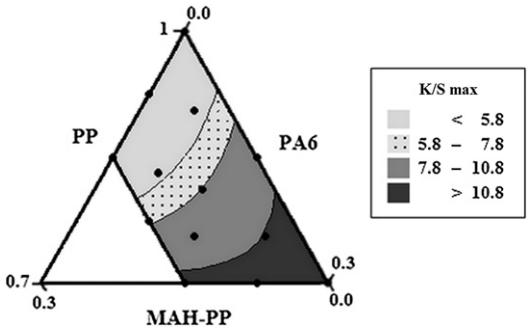

Fig. 11. Contour plot of the K/S_{max} model.

polyamide 6 to polypropylene causes coarse dispersed polyamide 6 particles having particle size greater than 2 microns within the PP matrix in sample 9 (Fig. 14c). But the particles become much finer with particle sizes less than 500 nanometers in sample 6 when 15% of the compatibilizer was added to the blend (Fig. 14d).

Variations in the elongation at break are also strongly dependent on the presence of the compatibilizer. This could also be explained in terms of formation of amide or imide linkages which induces interfacial bonding between polyamide 6 and polypropylene in the presence of MAH-PP. The compatibilized blends could withstand tensile deformation at a higher elongation at break because the interfacial adhesion between polyamide 6 and polypropylene is still strong enough to withstand the deformation up to its break point. Fig. 13 shows that the presence of 15% polyamide 6 in the PP matrix (sample 9), causes a decrement in the elongation at break from 2.38% for sample 4 to 1.91% for sample 9. By adding 15% of the compatibilizer, on the other hand the elongation at break increases to 3.93% (i.e. two times greater than 1.91%) for sample 6.

Although the K/S_{max} regression model emphasizes that both the polyamide 6 and the compatibilizer are significant for improving disperse dye uptake of the blends but it reveals that the presence of the polyamide 6 in the blends is more important than that of the compatibilizer. As Fig. 13 shows K/S_{max} of the neat PP sample (sample 4) is 1.14. By adding 15% of polyamide 6 to the neat PP (i.e. sample 9), the K/S_{max} increases to 9.67 i.e. 8.5 times greater than the K/S_{max} for the neat PP sample. When 15% of the compatibilizer is added (sample 6), however, the K/S_{max} of the sample is 11.39 i.e. an increase of only 1.18 times greater than the K/S_{max} of sample 9. It is clear then, that polyamide 6 has a more significant effect on the disperse dyeability of the blends than the compatibilizer. Principally, the dyeing process of a substrate is divided into four steps, namely: diffusion of dye in the dye bath solution, adsorption at the

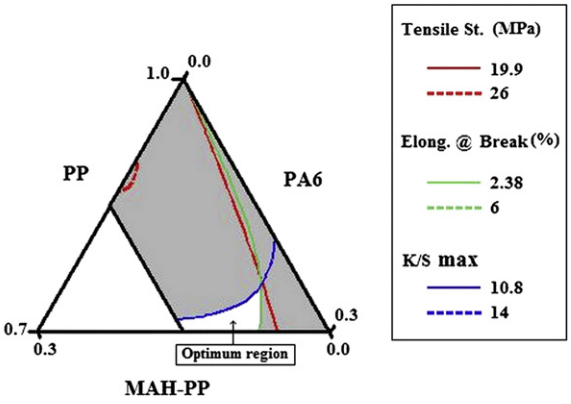

Fig. 12. Overlaid contour plot.

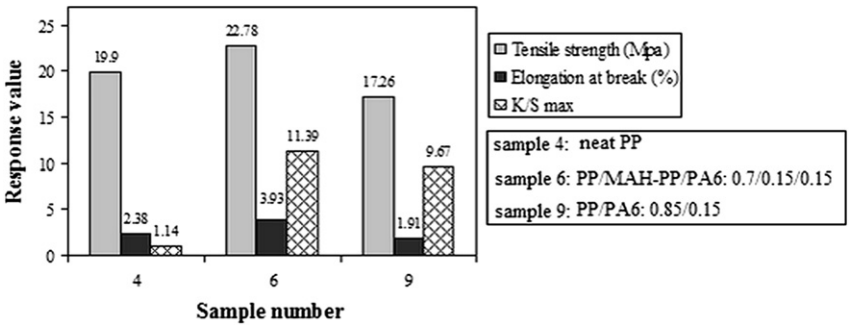

Fig. 13. Tensile strength, elongation at break and K/S_{max} for samples 4, 6 and 9.

substrate's surface, diffusion into the substrate and finally, fixation of the dye to the substrate. In order to achieve an acceptable dye uptake, it is necessary that the substrate should not only have sufficient amorphous regions for better dye diffusion but also it should possess enough polarity to encounter sufficient dye adsorption and good dye fixation during the dyeing process. It is well known that polypropylene has a non-polar, highly crystalline structure which limits the accessibility of dye molecules to its

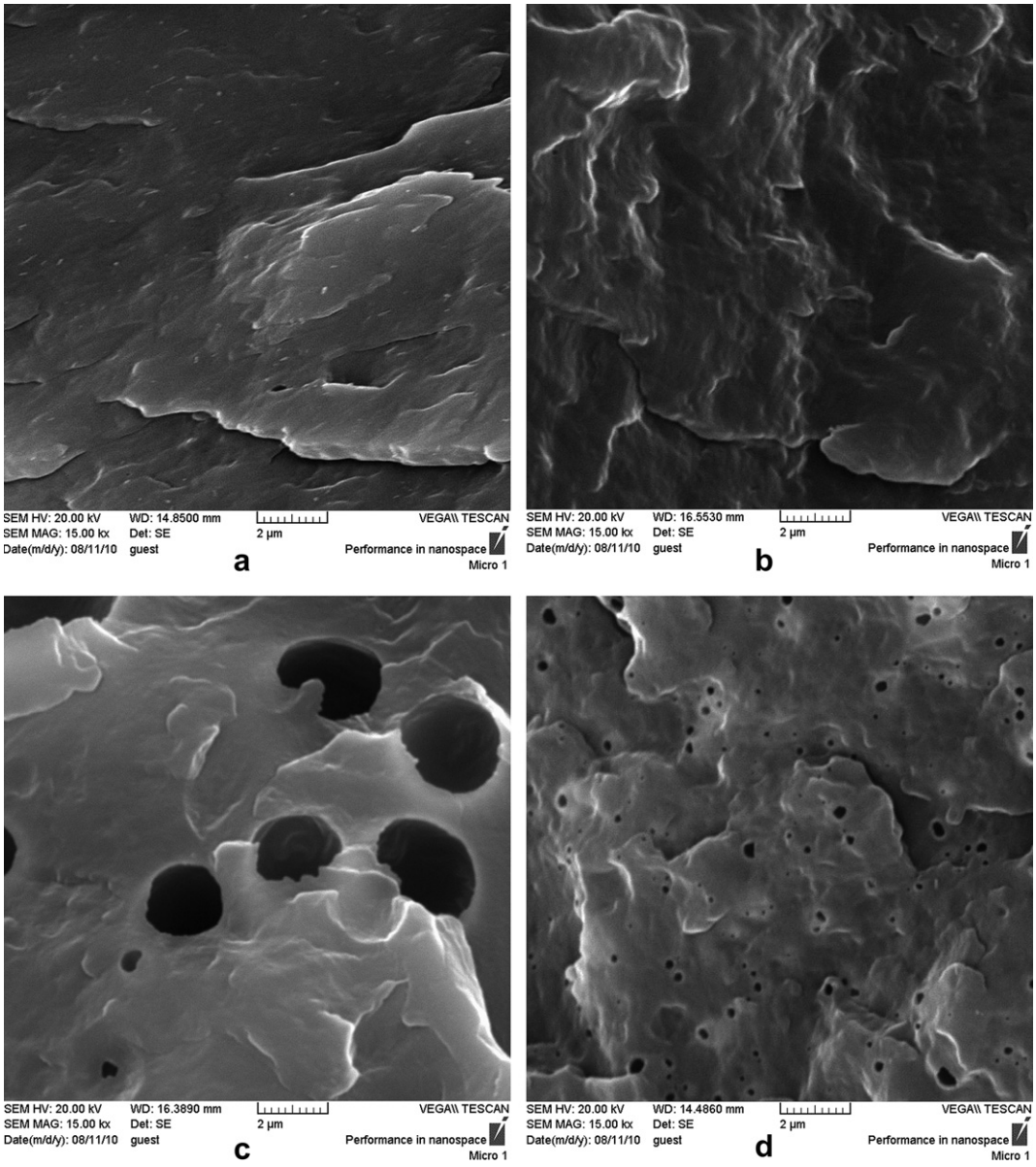

Fig. 14. SEM images of the blends, (a): PP; (b): PP/MAH-PP (0.85/0.15); (c): PP/PA6 (0.85/0.15); (d): PP/MAH-PP/PA6 (0.7/0.15/0.15).

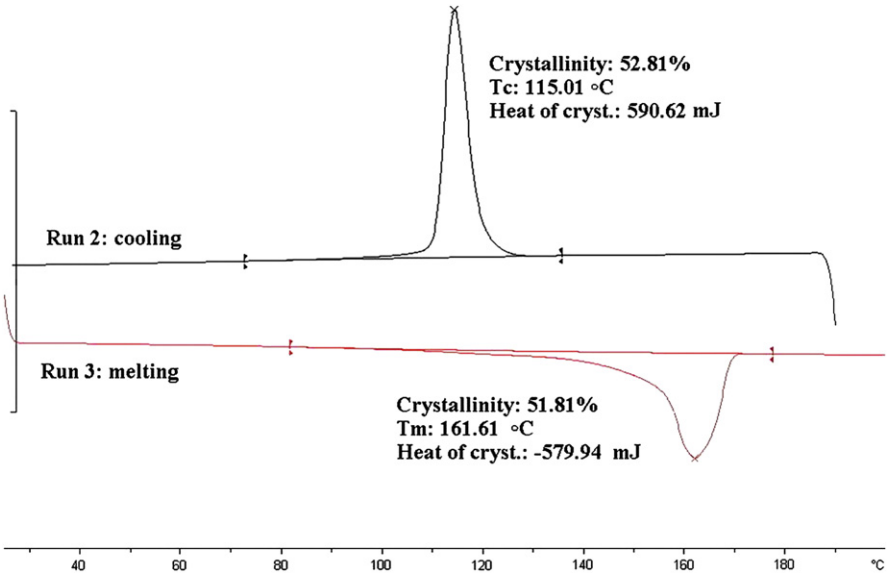

Fig. 15. DSC thermograph of sample 4 (neat PP).

matrix. Insufficient chemical affinity between the PP and dyes and lack of polarity of the polymer chains cause dye molecules to be retained only by weak non-polar physical forces. Also, the current theoretical knowledge about diffusion of a dyestuff from a solution into a substrate makes it possible to observe that disperse dyes diffuse primarily into the amorphous regions and the interfaces of a blend [11]. Therefore, it is no wonder that the K/S_{max} value for the disperse dyed neat PP sample is low (i.e. 1.14). Incorporation of the polyamide 6 into PP matrix results in creation of two distinct regions i.e. the polyamide 6 particulates and the interfacial regions in the blends. Both of these regions are susceptible to dyeing with disperse dyes. Table 2 indicates disperse dye uptake of Akulon F130 sample is 10.8. Adding of polyamide 6 into to the matrix which creates the interfacial regions in the blend, causes disperse dye uptake to increase e.g. to 9.67 for sample 9. DSC thermographs of Figs. 15 and 16 show the presence of the polyamide 6 in the matrix results in a slight decrease in the PP crystallinity. This could promote the diffusion of disperse dyes into the substrate. However, it is very important to note that incorporation of the compatibilizer into the blend makes finer polyamide 6 particulates and, therefore, a larger interfacial region will be formed. DSC thermographs of Figs. 16 and 17 show that during the cooling process of the PP/PA6 blend (run 2), two exothermic peaks appeared which are attributed to the crystallization of PA6 and PP components. However, during the cooling process of the PP/MAH-PP/PA6 blend, the PA6-related peak completely disappeared. This is attributed to the chemical interaction between MAH and NH2 groups approaching their maximal stoicheometric ratio, thereby forming amide or imide

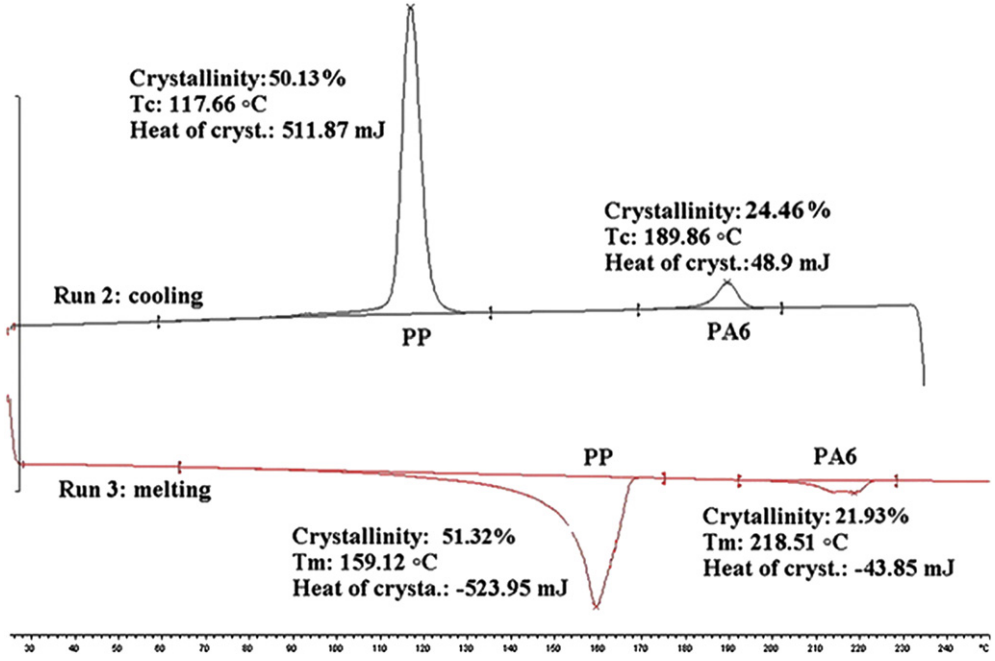

Fig. 16. DSC thermograph of sample 9 (PP/PA6: 0.85/0.15).

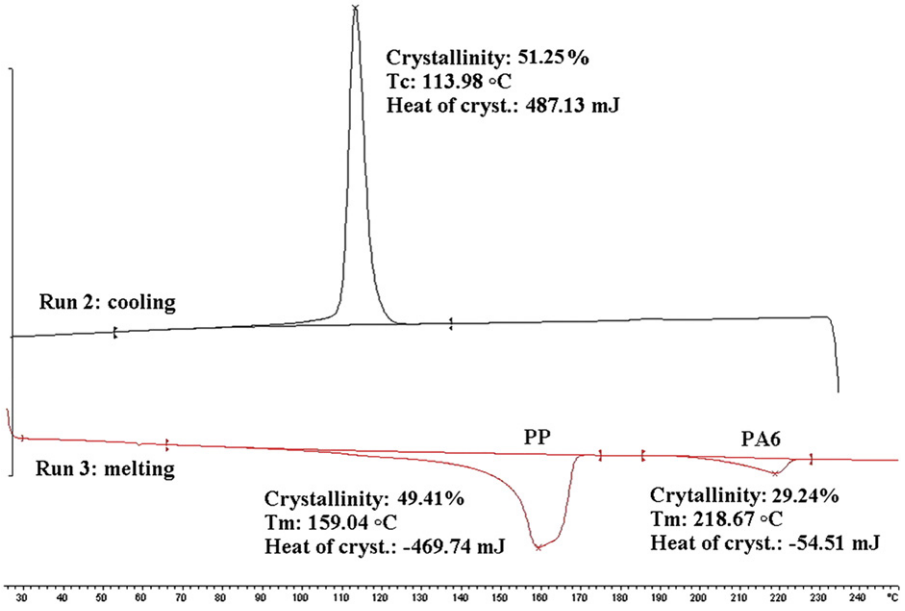

Fig. 17. DSC thermograph of sample 6 (PP/MAH-PP/PA6: 0.7/0.15/0.15).

Table 6
Fastness properties of various blended samples and pure polyamide 6 dyed with the disperse dye.

Samples	Proportion of the components			Wash Test 2, 50 °C ISO/R 105/IV, Part 9;			Rubbing ISO/R 105/I, Part 18;		XENON LAMP ISO/R 105/V, Part 2;
	PP	MAH-PP	PA6	Washing	Staining		With crockmeter		Assessment by blue scale
					CO	WO	Dry	Wet	
3	0.85	0.15	0	4 to 5	5	5	5	5	5
4	1	0	0	5	5	5	5	5	5
6	0.7	0.15	0.15	5	5	5	5	5	6
9	0.85	0	0.15	5	5	5	5	5	5 to 6
Akulon F130	(Pure polyamide 6)			4 to 5	5	5	5	5	6

linkages which suppress the crystallization of the PA6 component [26]. The DSC thermograph of Fig. 17 indicates that the compatibilizer causes the crystallinity of PP to decrease from 51.32% for sample 9 to 49.41% for sample 6. This could be due to the chemical interaction of the polyamide 6 with the PP matrix (i.e. the reaction between NH2 and MAH groups which results in formation of imide and amide linkages) which partially prevents the crystallization of the PP components. Therefore, because of increased interfacial regions as well as decreased PP crystallinity, the resultant disperse dye uptake increased from 9.67 for sample 9 to 11.39 for sample 6.

4.4. Wash, rub and light fastness properties

In order to assess the effect of each component on fastness properties of the blends, wash, rub and light fastnesses of samples 3, 4, 6, 9 and Akulon F130 (i.e. pure PA6) were determined by their respective standard test methods. Table 6 shows wash, rub and light fastnesses of these selected samples. All the selected samples have excellent wash and rub fastnesses and good light fastness similar to that of Akulon F130 (i.e. pure polyamide 6) sample. Therefore, because there is no significant difference between the fastness properties of the blends and that of the pure polyamide 6, it could be concluded that the other components have only a marginal effect on fastness properties of the blends.

5. Conclusions

The utilized experimental design provided varied predictive models for tensile strength, elongation at break and K/S_{max} with adequate goodness-of-fit. The tensile strength regression model illustrated that the compatiblizer (i.e. Fusabond® P MD353D) played an important role in improving the tensile properties and dyeability of the blends. Increased amounts of this compatiblizer resulted in finer dispersion of the polyamide 6 as well as increased formation of amide or imide linkages within the blend, hence enhancing the tensile strength of the resultant blends. Additionally, the formation of amide or imide linkages induce increased interfacial bonding between polyamide 6 and polypropylene which is reflected in improvements in the elongation at break.

The K/S_{max} regression model illustrated that the presence of polyamide 6 in the blend is essential for enhancing the dyeability of the blend. The addition of the compatiblizer, on the other hand, has a synergistic effect in disperse dye uptake of the resultant blends. Incorporation of polyamide 6 into the PP matrix created two distinct regions, namely the polyamide 6 particulates and the interfacial regions between the two polymers. These formed regions make the blend susceptible to dyeing with disperse dyes. The compatiblizer increased the number of the polyamide particulates, increased the interfacial regions as well as decreasing the

crystalinity of the blend and hence had a synergistic effect increasing the disperse dye uptake from 9.67 for sample 9 to 11.39 for sample 6. Overlaying the contour plots gave an optimum region for the proportions of the chosen components in which maximum disperse dye uptake as well as acceptable mechanical properties could be attained.

Fastness properties of the blends were good to excellent and comparable to the pure polyamide 6. The amount of each component did not have a significant effect on fastness properties of the blends.

Finally, despite high disperse dye uptake of most blends, the acid dye uptake as expected was unacceptable due to low amine content, weak basicity of the amine and high molecular weight of Akulon F130, the utilized polyamide 6.

Acknowledgements

The authors are indebted to Mr. Firooz Mazaheri for his guidance, provisions of dyestuffs and performance of fastness tests at technical laboratories of Ciba company Iran.

References

[1] Brydson JA. Plastics materials. Oxford: Butterworth-Heinemann; 1999.
[2] Kotek R, Afshari M, Gupta BS, Haghighat Kish M, Jung D. Polypropylene alloy filaments dyeable with disperse dyes. Color Technol 2004;120:26–9.
[3] Ahmed M. Polypropylene fibre: science and technology. Amsterdam: Elsevier Scientific Pub; 1982.
[4] Ataeefard M, Moradian S. Surface properties of polypropylene/organoclay nano-composites. Appl Surf Sci 2011;257:2320–6.
[5] Parvinzadeh M, Moradian S, Rashidi A, Yazdanshenas ME. Surface characterization of polyethylene terephthalate/silica nano-composites. Appl Surf Sci 2010;256:2792–802.
[6] Khatibzadeh M, Mohseni M, Moradian S. Compounding fibre grade polyethylene terephthalate with a hyperbranched additive and studying its dyeability with a disperse dye. Color Technol 2010;126:269–74.
[7] Son TW, Lim SK, Chang CM, Kim SS, Cho IS. Physical modification of polypropylene: preparation of fibres dyeable with disperse dyes. JSDC 1999;115:366–9.
[8] Hong S, Kim ST, Lee TS. Dyeing polypropylene fibres by means of copolymer additives. JSDC 1994;110:19–23.
[9] Mizutani Y, Nago S, Kawamura H. Dyeable polypropylene fiber. J Appl Polym Sci 1997;63:133–5.
[10] Seves A, De Marco T, Siciliano A, Martuscelli E, Marcandalli B. Blending polypropylene with hydrogenated oligocyclopentadiene: a new method for the production of dyeable fibers. Dyes Pigments 1995;28:19–29.
[11] Ujhelyiova A, Bolhova E, Oravkinova J, Tino R, Marcincin A. Kinetics of dyeing process of blend polypropylene/polyester fibres with disperse dye. Dyes Pigments 2007;72:212–6.
[12] Akrman J, Prikryl J. Dyeing behavior of polypropylene blend fiber. 1. Kinetic and thermodynamic parameters of the dyeing system. J Appl Polym Sci 1996;62:235–45.
[13] Akrman J, Prikryl J. Dyeing behavior of polypropylene blend fiber. II. Ionic exchange mechanism of dyeing. J Appl Polym Sci 1997;66:543–50.
[14] Akrman J, Kaplanova M. The coloration of polypropylene fibres with acid dyes. JSDC 1998;111:159–63.
[15] Akrman J, Prikryl J. Dyeing behavior of polypropylene blend fiber. III. Effect of drawing on dyeability. J Appl Polym Sci 1999;73:719–27.
[16] Seves A, Testa G, Marcandalli B, Bergamasco L, Munaretto G, Beltrame PL. Inducing water bath dyeability in polypropylene fibers by their blending with polyamide 6. Dyes Pigments 1997;35:367–73.
[17] Armstrong NA. Pharmaceutical experimental design and interpretation. Boca raton: Taylor & Francis Group; 2006.
[18] Cornell JA. Experiments with mixtures: designs, models, and the analysis of mixture data. John Wiley & Sons; 1990.
[19] Minitab® Release 15. Design of experiments, user's manual. Minitab Inc; 2007.
[20] Xiarchos I, Jaworskab A, Zakrzewska-Trznadel G. Response surface methodology for the modelling of copper removal from aqueous solutions using micellar-enhanced ultrafiltration. J Membr Sci 2008;321:222–31.
[21] Cochran WG, Cox GM. Experimental designs. 2nd ed. New York: John Wiley & Sons; 1992.
[22] Myers RH, Montgomery DC. Response surface methodology: process and product optimization using designed experiments. 2nd ed. New York: John Wiley & Sons; 2002.
[23] Vasile C. Handbook of polyolefins. 2nd ed. Marcel Dekker; 2000.
[24] Tavanai H, Morshed M, Hosseini SM. Effects of on-line melt blending of polypropylene with polyamide 6 on the bulk and strength of the resulting BCF yarn. Iran Polym J 2003;12:421–30.
[25] Tucker JD, Lee S, Einsporn RL. A study of the effect of PP-g-MA and SEBS-g-MA on the mechanical and morphological properties of polypropylene/nylon 6 blends. Polym Eng Sci 2000;40:2577–89.
[26] Takahashi T. Effect of maleic anhydride grafted polypropylene on structure of polypropylene/polyamide 6 blend fiber. Sen'I Gakkaishi 2002;58:238–47.
[27] Moad G. The synthesis of polyolefin graft copolymers by reactive extrusion. Prog Polym Sci 1999;24:81–142.